SUPPLEMENTARY ONLINE MATERIAL

Sample descriptions and analytical methods. NMB-03-1, the North Mtn. Basalt, was collected at the location described in Schoene et al. (2006) and Hodych and Dunning (1992). It comes from pegmatitic segregations within the lowest basaltic flow, which were interpreted by Greenough and Dostal (1992) to have formed *in situ* after eruption of the basalt, and therefore zircon dates from these segregations very closely date the eruption (further description of the NMB is found in Kontak; 2008). Our sample was processed at MIT using standard crushing and mineral separation procedure. It yielded abundant stubby prismatic grains from which single grains were selected for chemical abrasion. Ash sample NYC-N10 was taken from the New York canyon section, Nevada, USA, whose location is described in Guex et al. (2004) and Ward et al. (2007). The GPS location for *P. spelae* in this section is N 38˚29'10.6", W 118˚05'0.72". The other ash samples come from the Pucara Group sediments in the Utcubamba Valley, Northern Peru, which is described in Schaltegger et al. (2008). The GPS location for P. spelae in this section is S 06˚18'28.5", W 77˚53'16.2". Sampled ash beds were between 1 and 7 cm thick and consisted of gray to green to yellow fine-grained material. Ashes were processed at UNIGE by first crushing with a hammer in a plastic bag and then placed in a tungsten mill shatterbox for five second increments and sieved to <500 μm. Separated material was then washed with water in a large beaker and decanted multiple times to remove clay material, and the resulting separates were put through magnetic and heavy liquid separation. This resulted in between 100 (LM4-100/101) and 20 zircons (NYC-N10). Single grains were picked for chemical abrasion and combined in a quartz beaker

for annealing at 900 ˚C for ~60 hours. All grains from a single sample were leached together in 3 ml savillex beakers in HF + trace HNO_3 for ~12 hours, rinsed with water and acetone and then placed in 6N HCl on a hotplate at ~110 ˚C overnight. These were then washed several times with water, HCl, and HNO_3. Single grains were then handpicked for dissolution, which varied from short and stubby to long and prismatic with variable levels of clarity. There was no obvious correlation between grain morphology and age in any of the analyzed samples, though youngest ash zircons were always long and prismatic. Each grain was spiked with ~0.004 g of the EARTHTIME ($\pm^{202}$Pb)-^{205}Pb-^{233}U-^{235}U tracer solution. Zircons were dissolved in ~70 µl 40% HF and trace HNO_3 in 200 µl savillex capsules at 210 ˚C for 48+ hours, dried down and redissolved in 6N HCl overnight. Samples were then dried down and redissolved in 3N HCl and put through a modified single 50 µl column anion exchange chemistry (Krogh, 1973). U and Pb were collected in the same beaker and dried down with a drop of 0.05 M H_3PO_4, and analyzed on a single outgassed Re filament in a Si-gel emitter, modified from Gerstenberger and Haas (Gerstenberger and Haase, 1997). Measurements were performed on a Thermo-Finigan Triton thermal ionization mass spectrometer at UNIGE and a VG S54 thermal ionization mass spectrometer at MIT.

On the Triton, Pb was measured in dynamic mode on a modified Masscom secondary electron multiplier (SEM). Deadtime for the SEM was determined by periodic measurement of NBS-982 for up to 1.3 Mcps and observed to be constant at 23.5 ns. Multiplier linearity was monitored every few days between $1.3x10^6$ and <100 cps by a combination of measurements of NBS-981, -982 and -983, and observed to be constant if the Faraday to SEM yield was kept between ~93-94% by adjusting SEM voltage.

Baseline measurements were made at masses 203.5 and 204.5 and the average was subtracted from each peak after beam decay correction. Interferences on ^{202}Pb and ^{205}Pb were monitored by measuring masses 201 and 203 and also by monitoring masses 202 and 205 in unspiked samples. As a result, no corrections were applied. For samples with the ^{202}Pb-^{205}Pb-^{233}U-^{235}U tracer each measured ratio was corrected for fractionation in the data acquisition software using a $^{202}Pb/^{205}Pb$ of 0.99989. For single-Pb spike samples, the average fractionation value determined by the ^{202}Pb-^{205}Pb tracer was used, and this was 0.13±0.04 (2-sigma standard deviation).

On the Triton U was measured in static mode on Faraday cups and 10^{12} ohm resistors as UO_2^+. Oxygen isotopic composition was monitored by measurement of mass 272 on large U500 loads (Wasserburg et al., 1981). Though the $^{18}O/^{16}O$ typically grew from 0.00200 to 0.00208 over the course of an analysis, the most drastic increase occurred at the beginning towards an average value of ~0.00205. As a result, early blocks of data were deleted and the average value was used for all data, and corrected during mass spectrometry. Baselines were measurement at ±0.5 mass units for 30 seconds every 50 ratios. Correction for mass-fractionation for U was done with the double spike assuming a sample $^{238}U/^{235}U$ ratio of 137.88. Measured ratios were reduced using the algorithms of Schmitz and Schoene (2007) and Crowley et al. (2007) (Supplementary Table 1), using the following tracer composition, which has a $^{235}U/^{205}Pb$ = 100.20 to which a total uncertainty of 0.1 was assigned (Supplementary Table 2).

All ashbed zircons were measured at UNIGE. Because many of the tuff zircons in this study are very low-U, the largest uncertainty in the calculated date is that of the correction for common lead. We measured over 40 total procedural blanks at UNIGE

over the course of this study, spiked either the tracer containing ^{202}Pb or with the single Pb tracer. We found that the amount of common Pb in blanks agreed well with that found in zircon analyses, suggesting all common Pb came from blank. The tracer-stripped isotopic composition resulting from each tracer was slightly different, and this is likely due to different isotopic compositions in the tracers themselves. Thus, zircons analyzed with ^{205}Pb-^{233}U-^{235}U were reduced using the corresponding blank composition and vice versa. After 2-sigma outlier rejection, the composition of fifteen ^{205}Pb-^{233}U-^{235}U -spiked blanks was: ^{206}Pb/^{204}Pb = 18.08±0.66, ^{207}Pb/^{204}Pb = 15.79±0.45, ^{208}Pb/^{204}Pb = 37.55±0.93 (2-sigma standard deviations) and for 27 ^{202}Pb-^{205}Pb-^{233}U-^{235}U -spiked blanks was: ^{206}Pb/^{204}Pb = 18.39±0.22, ^{207}Pb/^{204}Pb = 15.62±0.20, ^{208}Pb/^{204}Pb = 37.62±0.78 (2-sigma standard deviations). To test the accuracy of the ^{202}Pb-^{205}Pb-^{233}U-^{235}U composition, we intentionally picked very small fragments (<20 μm diameter) of North Mtn. Basalt (NMB-03-1) in order to achieve similar ratios of radiogenic Pb to blank Pb as those observed in ash bed zircons. Because this did not introduce scatter into the results, we conclude the blank composition is approximately correct, and not the cause of the range in dates seen in each ash bed. Blank calculation at MIT followed a similar procedure, and resulted in the following composition, used to reduce all NMB-03-1 data: ^{206}Pb/^{204}Pb = 18.30±0.26, ^{207}Pb/^{204}Pb = 15.38±0.17, ^{208}Pb/^{204}Pb = 37.45±0.72.

References cited (for Supplementary text)

Crowley, J.L., Schoene, B., and Bowring, S.A., 2007, U-Pb dating of zircon in the Bishop Tuff at the millennial scale: Geology, v. 35, p. 1123-1126; doi: 10.1130/G24017A.

Gerstenberger, H., and Haase, G., 1997, A highly effective emitter substance for mass spectrometric Pb isotope ratio determinations: Chemical Geology, v. 136, p. 309-312.

Greenough, J.D., and Dostal, J., 1992, Cooling history and differentiation of a thick North Mountain Basalt flow (Nova Scotia, Canada): Bulletin of Volcanology, v. 55, p. 63-73.

Guex, J., Bartolini, A., Atudorei, V., and Taylor, D., 2004, High-resolution ammonite and carbon isotope stratigraphy across the Triassic-Jurassic boundary at New York Canyon (Nevada): Earth and Planetary Science Letters, v. 225, p. 29-41.

Hodych, J.P., and Dunning, G.R., 1992, Did the Manicouagan impact trigger end-of-Triassic mass extinction?: Geology, v. 20, p. 21-54.

Jaffey, A.H., Flynn, K.F., Glendenin, L.E., Bentley, W.C., and Essling, A.M., 1971, Precision measurement of half-lives and specific activities of ^{235}U and ^{238}U: Physical Review, v. C4, p. 1889-1906.

Kontak, D.J., 2008, On the edge of CAMP: Geology and volcanology of the Jurassic North Mountain Basalt, Nova Scotia: Lithos, v. 101, p. 74-10; doi:10.1016/j.lithos.2007.07.013.

Krogh, T.E., 1973, A low contamination method for hydrothermal decomposition of zircon and extraction of U and Pb for isotopic age determination: Geochimica et Cosmochimica Acta, v. 37, p. 485-494.

Schaltegger, U., Guex, J., Bartolini, A., Schoene, B., and Ovtcharova, M., 2008, Precise U-Pb age constraints for end-Triassic mass extinction, its correlation to volcanism and Hettangian post-extinction recovery: Earth and Planetary Science Letters, v. 267, p. 266-275, doi:10.1016/j.epsl.2007.11.031.

Schmitz, M.D., and Schoene, B., 2007, Derivation of isotope ratios, errors, and error correlations for U-Pb geochronology using 205Pb-235U-(233U)-spike isotope dilution thermal ionization mass spectrometric data: Geochemistry, Geophysics, Geosystems, v. 8, p. Q08006, doi: 10.1029/2006GC001492.

Schoene, B., Crowley, J.L., Condon, D.C., Schmitz, M.D., and Bowring, S.A., 2006, Reassessing the uranium decay constants for geochronology using ID-TIMS U-Pb data: Geochimica et Cosmochimica Acta, v. 70, p. 426-445.

Ward, P.D., Garrison, G.H., Williford, K.H., Kring, D.A., Goodwin, D., Beattie, M.J., and McRoberts, C.A., 2007, The organic carbon isotopic and paleontological record across the Triassic-Jurassic boundary at the candidate GSSP section at Ferguson Hill, Muller Canyon, Nevada, USA: Palaeogeography, Palaeoclimatology, Palaeoecology, v. 244, p. 281-289.

Wasserburg, G.J., Jacousen, S.B., DePaolo, D.J., McCulloch, M.T., and Wen, T., 1981, Precise determinations of Sm/Nd ratios, Sm and Nd isotopic abundances in standard solutions: Geochimica Cosmochimica Acta, v. 45, p. 2311-2323.

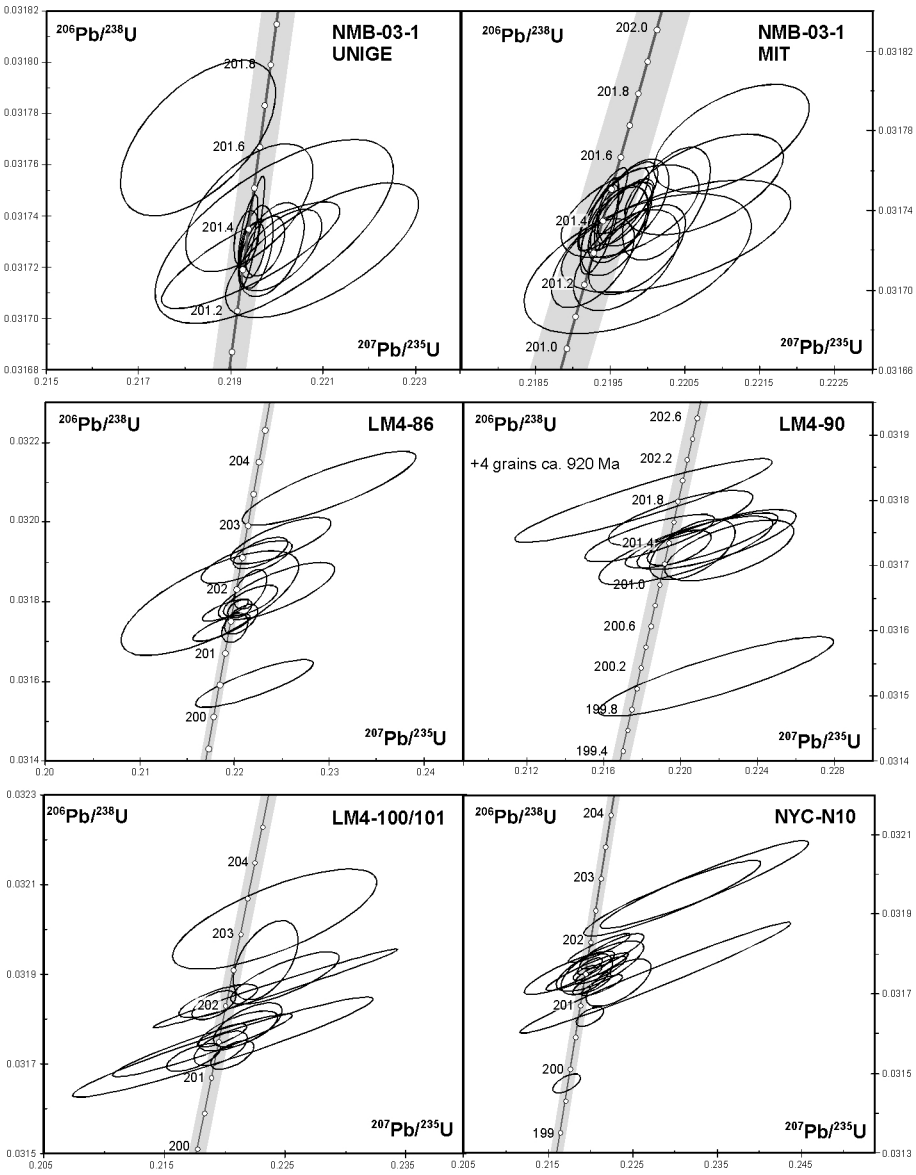

Supplementary Fig. 1. Concordia plots for samples from this study. Uncertainties are at the 95% confidence level and were calculated using the algorithms in Crowley et al. (2007) and Schmitz and Schoene (2007).

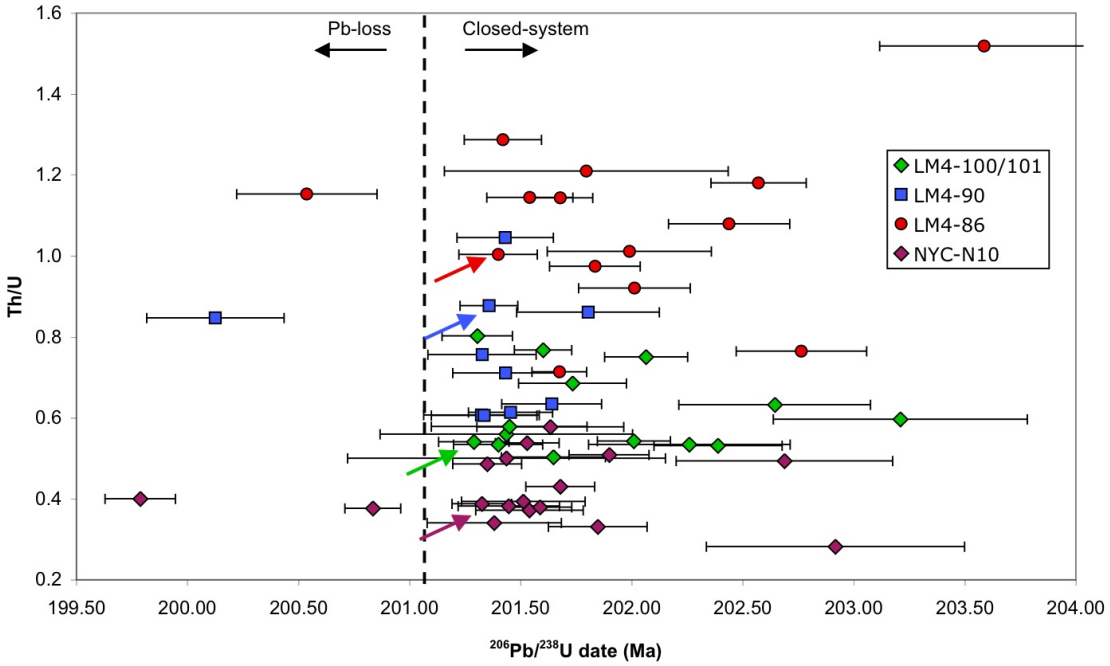

Supplementary Fig. 2: Th/U ratio plotted versus age (Supplementary Table 3) for each single zircon analysis. Th/U from each sample form overlapping clusters, and the average Th/U of zircons from the each Pucara sample decrease with increasing stratigraphic height. The youngest zircon from each sample (indicated by color-coded arrows), chosen as the eruption age, follow this same trend. The overlap in populations may be evidence of zircon inheritance and recycling from older batches of magma or host rocks.

Supplementary Table 1: U-Pb ID-TIMS isotopic data

						Radiogenic Isotope Ratios								Isotopic Ages					
Sample	tracer	$\frac{Th}{U}$	$\frac{Pb^*}{Pb_c}$	Pb_c (pg)	$\frac{^{206}Pb}{^{204}Pb}$	$\frac{^{208}Pb}{^{206}Pb}$	$\frac{^{207}Pb}{^{206}Pb}$	% err	$\frac{^{207}Pb}{^{235}U}$	% err	$\frac{^{206}Pb}{^{238}U}$	% err	corr. coef.	$\frac{^{207}Pb}{^{206}Pb}$	±	$\frac{^{207}Pb}{^{235}U}$	±	$\frac{^{206}Pb}{^{238}U}$	±
(a)	(b)	(c)	(d)	(d)	(e)	(f)	(f)	(g)	(f)	(g)	(f)	(g)		(h)	(g)	(h)	(g)	(h)	(g)
NMB-03-1 (MIT)																			
z48	ET535	2.855	87	0.46	3232	0.908	0.050145	0.178	0.219272	0.206	0.031714	0.057	0.592	201.74	4.14	201.30	0.38	201.27	0.11
z49	ET535	1.834	39	0.42	1740	0.585	0.050281	0.525	0.219868	0.567	0.031714	0.092	0.523	208.03	12.18	201.80	1.04	201.27	0.18
z51	ET535	1.595	58	1.16	2701	0.508	0.050248	0.235	0.219729	0.265	0.031715	0.066	0.544	206.50	5.46	201.68	0.48	201.27	0.13
z44	ET535	1.475	49	1.17	2354	0.470	0.050261	0.226	0.219825	0.253	0.031721	0.058	0.560	207.06	5.23	201.76	0.46	201.31	0.11
z38	ET535	1.245	105	1.04	5290	0.396	0.050202	0.108	0.219603	0.146	0.031726	0.070	0.710	204.37	2.51	201.58	0.27	201.34	0.14
z43	ET535	1.472	23	1.02	1127	0.470	0.050378	0.529	0.220381	0.568	0.031727	0.074	0.571	212.49	12.26	202.23	1.04	201.35	0.15
z68	ET535	2.161	198	0.50	8240	0.687	0.050147	0.080	0.219395	0.117	0.031730	0.057	0.788	201.83	1.87	201.41	0.21	201.37	0.11
z67	ET535	1.167	88	0.66	4498	0.371	0.050196	0.137	0.219609	0.168	0.031731	0.061	0.641	204.09	3.17	201.58	0.31	201.37	0.12
z70	ET535	1.811	237	0.48	10553	0.576	0.050152	0.073	0.219415	0.112	0.031731	0.058	0.814	202.03	1.69	201.42	0.20	201.37	0.12
z36	ET535	2.084	99	0.43	4183	0.663	0.050193	0.142	0.219632	0.170	0.031736	0.052	0.643	203.95	3.30	201.60	0.31	201.40	0.10
z28	ET535	2.281	107	0.63	4387	0.726	0.050203	0.129	0.219682	0.157	0.031737	0.050	0.668	204.39	2.99	201.64	0.29	201.41	0.10
z35	ET535	2.313	42	0.88	1703	0.737	0.050219	0.316	0.219771	0.345	0.031740	0.059	0.552	205.13	7.33	201.72	0.63	201.43	0.12
z52	ET535	2.086	94	0.43	3976	0.664	0.050171	0.148	0.219565	0.177	0.031740	0.057	0.627	202.90	3.43	201.55	0.32	201.43	0.11
z37	ET535	2.135	216	0.58	9030	0.679	0.050142	0.077	0.219443	0.113	0.031741	0.054	0.803	201.57	1.78	201.45	0.21	201.44	0.11
z26	ET535	2.145	112	0.39	4695	0.683	0.050193	0.136	0.219690	0.165	0.031744	0.055	0.648	203.95	3.16	201.65	0.30	201.46	0.11
z29	ET535	1.888	270	0.32	11823	0.600	0.050169	0.059	0.219584	0.097	0.031744	0.048	0.882	202.83	1.38	201.56	0.18	201.46	0.10
z27	ET535	2.188	82	0.42	3410	0.698	0.050324	0.190	0.220263	0.222	0.031744	0.075	0.572	209.98	4.39	202.13	0.41	201.46	0.15
z45	ET535	1.930	81	0.78	3537	0.615	0.050219	0.152	0.219806	0.180	0.031745	0.052	0.627	205.14	3.54	201.75	0.33	201.46	0.10
z42	ET535	1.862	33	0.74	1474	0.595	0.050413	0.379	0.220719	0.411	0.031754	0.064	0.551	214.08	8.78	202.51	0.75	201.52	0.13
z34	ET535	2.444	49	0.34	1945	0.782	0.050468	0.349	0.221120	0.381	0.031777	0.069	0.537	216.61	8.08	202.84	0.70	201.66	0.14

NMB-03-1 (UNIGE)

z6	ET2535	1.837	12	2.02	565	0.584	0.050160	0.680	0.219416	0.724	0.031725	0.053	0.828	202.42	15.79	201.42	1.32	201.34	0.11
z3	ET2535	1.853	100	0.92	4446	0.590	0.050171	0.092	0.219473	0.101	0.031727	0.028	0.461	202.92	2.13	201.47	0.18	201.35	0.06
z2	ET2535	1.355	24	0.85	1177	0.432	0.050303	0.324	0.220053	0.347	0.031727	0.041	0.586	209.04	7.52	201.95	0.64	201.35	0.08
z7	ET2535	1.094	10	2.46	519	0.350	0.050505	0.728	0.220935	0.776	0.031727	0.069	0.714	218.30	16.86	202.69	1.43	201.35	0.14
z5	ET2535	1.989	43	0.62	1896	0.634	0.050267	0.241	0.219899	0.260	0.031727	0.047	0.479	207.37	5.59	201.83	0.48	201.35	0.09
z11	ET2535	2.498	83	0.32	3276	0.795	0.050182	0.132	0.219532	0.146	0.031728	0.042	0.463	203.44	3.07	201.52	0.27	201.36	0.08
z4	ET2535	1.920	64	1.30	2806	0.612	0.050230	0.143	0.219744	0.154	0.031728	0.030	0.472	205.66	3.31	201.70	0.28	201.36	0.06
z1	ET2535	2.011	219	0.85	9473	0.640	0.050145	0.043	0.219392	0.053	0.031731	0.027	0.588	201.73	1.01	201.40	0.10	201.38	0.05
z10	ET2535	1.978	106	1.18	4609	0.629	0.050129	0.080	0.219321	0.089	0.031732	0.027	0.469	200.96	1.85	201.34	0.16	201.38	0.05
z9	ET2535	2.012	181	0.97	7799	0.640	0.050146	0.056	0.219400	0.075	0.031732	0.046	0.666	201.79	1.30	201.41	0.14	201.38	0.09
z16	ET2535	2.636	12	0.54	483	0.840	0.050268	0.895	0.219948	0.955	0.031734	0.093	0.667	207.42	20.77	201.87	1.75	201.39	0.18
z12	ET2535	1.998	258	0.46	11145	0.636	0.050168	0.039	0.219575	0.052	0.031743	0.033	0.680	202.79	0.89	201.56	0.10	201.45	0.07
z15	ET2535	2.273	20	0.70	842	0.722	0.050124	0.487	0.219387	0.521	0.031744	0.064	0.567	200.77	11.31	201.40	0.95	201.45	0.13
z17	ET2535	3.096	19	0.57	689	0.979	0.049835	0.589	0.218309	0.630	0.031771	0.079	0.562	187.32	13.71	200.50	1.15	201.62	0.16

LM4-86 (UNIGE)

z27	ET2535	1.153	4	0.74	212	0.373	0.050984	2.144	0.222118	2.281	0.031597	0.160	0.862	240.10	49.4	203.67	4.21	200.54	0.32
z26	ET2535	1.004	7	0.56	381	0.318	0.049973	1.053	0.218663	1.121	0.031735	0.089	0.773	193.73	24.5	200.80	2.04	201.40	0.18
z12	ET535	1.287	18	0.69	937	0.410	0.050285	0.493	0.220052	0.536	0.031739	0.088	0.552	208.18	11.4	201.95	0.98	201.42	0.17
z10	ET535	1.145	13	1.41	701	0.366	0.050389	0.597	0.220641	0.647	0.031758	0.098	0.560	212.95	13.8	202.44	1.19	201.54	0.19
z23	ET2535	0.714	15	0.71	888	0.228	0.050330	0.459	0.220532	0.491	0.031779	0.062	0.559	210.25	10.6	202.35	0.90	201.67	0.12
z28	ET2535	1.143	9	0.76	468	0.363	0.049993	0.844	0.219062	0.899	0.031780	0.074	0.751	194.69	19.6	201.13	1.64	201.68	0.15
z16	ET535	1.210	2	1.07	139	0.381	0.049563	3.394	0.217306	3.611	0.031799	0.321	0.698	174.57	79.2	199.67	6.54	201.80	0.64
z24	ET2535	0.975	7	0.68	405	0.312	0.050544	0.993	0.221650	1.059	0.031805	0.103	0.671	220.10	23.0	203.28	1.95	201.83	0.20
z19	ET2535	1.012	4	0.55	214	0.327	0.051138	2.104	0.224428	2.240	0.031830	0.186	0.750	247.05	48.4	205.59	4.17	201.99	0.37
z11	ET535	0.921	13	1.28	726	0.295	0.050489	0.593	0.221604	0.647	0.031833	0.126	0.508	217.55	13.7	203.24	1.19	202.01	0.25
z20	ET2535	1.079	4	1.10	242	0.344	0.050324	1.663	0.221354	1.769	0.031902	0.137	0.793	209.98	38.5	203.04	3.26	202.44	0.27
z17	ET535	1.180	14	0.41	755	0.378	0.050608	0.954	0.222751	1.022	0.031923	0.107	0.660	223.01	22.1	204.20	1.89	202.57	0.21
z22	ET2535	0.765	4	1.16	222	0.247	0.051050	1.796	0.224916	1.912	0.031954	0.147	0.808	243.10	41.4	205.99	3.57	202.76	0.29
z25	ET2535	1.519	3	0.96	140	0.498	0.051952	3.011	0.229830	3.209	0.032085	0.234	0.852	283.28	68.9	210.06	6.09	203.59	0.47

LM4-90 (UNIGE)

z12	ET2535	0.847	4	0.58	229	0.274	0.051021	2.138	0.221818	2.274	0.031531	0.157	0.876	241.80	49.3	203.42	4.19	200.13	0.31
z11	ET2535	0.607	4	0.80	265	0.194	0.050350	1.568	0.220230	1.669	0.031723	0.131	0.780	211.18	36.3	202.10	3.06	201.32	0.26
z4	ET2535	0.757	6	0.75	339	0.244	0.050870	1.146	0.222507	1.222	0.031724	0.123	0.653	234.93	26.4	203.99	2.26	201.33	0.24
z10	ET2535	0.607	10	0.40	626	0.194	0.050439	0.747	0.220632	0.801	0.031725	0.120	0.514	215.26	17.3	202.44	1.47	201.34	0.24
z8	ET2535	0.877	13	0.62	717	0.280	0.050273	0.581	0.219933	0.620	0.031729	0.066	0.623	207.65	13.5	201.85	1.14	201.36	0.13
z3	ET2535	1.045	5	1.19	296	0.335	0.050511	1.380	0.221052	1.468	0.031740	0.110	0.818	218.56	31.9	202.78	2.70	201.43	0.22
z2	ET2535	0.711	5	1.46	290	0.228	0.050699	1.434	0.221880	1.527	0.031740	0.120	0.789	227.19	33.1	203.47	2.81	201.43	0.24
z15	ET2535	0.614	6	0.70	385	0.194	0.049905	1.212	0.218426	1.288	0.031744	0.095	0.814	190.55	28.2	200.60	2.34	201.45	0.19
z13	ET2535	0.635	6	0.61	371	0.202	0.050234	1.323	0.220074	1.408	0.031774	0.113	0.765	205.84	30.7	201.97	2.58	201.64	0.23
z1	ET2535	0.862	3	1.80	176	0.272	0.049729	2.385	0.218042	2.533	0.031800	0.162	0.920	182.37	55.6	200.28	4.60	201.80	0.32
z14	ET2535	0.522	17	0.62	998	0.160	0.069613	0.308	1.469497	0.415	0.153101	0.247	0.676	916.96	6.3	917.92	2.51	918.32	2.11
z5	ET2535	0.566	9	0.63	573	0.174	0.070359	0.539	1.486947	0.597	0.153277	0.116	0.570	938.84	11.0	925.07	3.62	919.31	0.99
z9	ET2535	0.502	49	0.42	2906	0.154	0.070008	0.100	1.487183	0.117	0.154069	0.041	0.540	928.60	2.1	925.17	0.71	923.73	0.36
z7	ET2535	0.473	13	0.81	809	0.145	0.070208	0.342	1.496745	0.478	0.154619	0.302	0.700	934.43	7.0	929.06	2.91	926.80	2.61

LM4-100/101 (UNIGE)

z16	ET2535	0.541	8	0.66	477	0.171	0.049735	0.842	0.217501	0.897	0.031718	0.080	0.704	182.62	19.6	199.83	1.63	201.29	0.16
z7	ET2535	0.803	13	0.53	770	0.257	0.050446	0.638	0.220630	0.681	0.031720	0.080	0.583	215.61	14.8	202.43	1.25	201.30	0.16
z12	ET2535	0.535	9	0.81	562	0.170	0.050194	0.768	0.219630	0.821	0.031735	0.101	0.567	203.98	17.8	201.60	1.50	201.40	0.20
z17	ET2535	0.560	1	2.18	102	0.178	0.050238	4.363	0.219865	4.638	0.031741	0.287	0.959	206.03	101.2	201.80	8.49	201.44	0.57
z9	ET2535	0.578	2	1.01	166	0.183	0.049842	2.665	0.218144	2.832	0.031743	0.177	0.945	187.61	62.0	200.36	5.15	201.45	0.35
z13	ET2535	0.768	9	0.96	538	0.244	0.050170	0.733	0.219749	0.780	0.031768	0.065	0.746	202.87	17.0	201.70	1.43	201.60	0.13
z15	ET2535	0.503	6	0.45	379	0.161	0.050470	1.129	0.221116	1.203	0.031775	0.118	0.663	216.70	26.1	202.84	2.21	201.65	0.23
z4	ET2535	0.686	7	0.61	423	0.220	0.050626	1.003	0.221898	1.076	0.031789	0.122	0.634	223.86	23.2	203.49	1.98	201.73	0.24
z18	ET2535	0.543	10	0.57	618	0.172	0.049919	0.639	0.219100	0.683	0.031833	0.083	0.571	191.21	14.9	201.16	1.25	202.01	0.16
z8	ET2535	0.751	7	0.51	402	0.238	0.049982	1.144	0.219440	1.217	0.031842	0.094	0.792	194.17	26.6	201.44	2.22	202.07	0.19
z10	ET2535	0.534	2	2.60	118	0.173	0.051022	3.514	0.224223	3.738	0.031873	0.228	0.986	241.82	81.0	205.42	6.95	202.26	0.45
z3	ET535	0.531	4	0.94	262	0.172	0.051169	1.518	0.225014	1.622	0.031894	0.145	0.743	248.44	34.9	206.07	3.03	202.39	0.29
z1	ET535	0.633	9	1.05	568	0.203	0.050732	0.948	0.223381	1.033	0.031934	0.217	0.479	228.68	21.9	204.72	1.91	202.64	0.43
z5	ET535	0.597	2	2.00	149	0.192	0.050743	2.913	0.224059	3.105	0.032025	0.286	0.699	229.15	67.3	205.28	5.77	203.21	0.57

NYC-N10 (UNIGE)

z15	ET2535	0.400	12	0.51	761	0.127	0.050033	0.543	0.217149	0.582	0.031477	0.081	0.533	196.55	12.6	199.53	1.05	199.79	0.16
z7	ET2535	0.377	10	1.10	649	0.120	0.050387	0.597	0.219848	0.637	0.031645	0.064	0.657	212.88	13.8	201.78	1.17	200.83	0.13
z12	ET2535	0.388	7	1.15	447	0.125	0.050639	0.848	0.221498	0.903	0.031723	0.068	0.822	224.44	19.6	203.16	1.66	201.33	0.13
z16	ET2535	0.486	8	0.64	498	0.155	0.050322	0.809	0.220136	0.862	0.031727	0.078	0.706	209.89	18.7	202.02	1.58	201.35	0.15
z10	ET2535	0.341	5	0.53	331	0.110	0.051045	1.303	0.223335	1.392	0.031732	0.153	0.620	242.87	30.0	204.68	2.58	201.38	0.30
z3	ET2535	0.500	1	3.33	82	0.165	0.052044	5.383	0.227771	5.737	0.031741	0.361	0.982	287.37	123.0	208.36	10.81	201.44	0.72
z6	ET2535	0.383	11	0.61	690	0.121	0.049967	0.692	0.218690	0.743	0.031743	0.115	0.503	193.46	16.1	200.82	1.35	201.45	0.23
z5	ET2535	0.393	3	1.30	217	0.124	0.049684	1.912	0.217521	2.032	0.031753	0.140	0.870	180.22	44.5	199.84	3.69	201.51	0.28
z18	ET2535	0.539	11	0.43	669	0.171	0.050187	0.604	0.219746	0.645	0.031756	0.073	0.604	203.67	14.0	201.70	1.18	201.53	0.14
z1	ET2535	0.372	4	1.09	242	0.118	0.050170	1.727	0.219680	1.837	0.031758	0.122	0.907	202.86	40.1	201.64	3.36	201.54	0.24
z9	ET2535	0.379	7	0.52	484	0.121	0.050340	0.801	0.220478	0.854	0.031765	0.072	0.745	210.71	18.6	202.31	1.57	201.59	0.14
z4	ET2535	0.578	4	1.04	245	0.185	0.050495	1.858	0.221208	1.979	0.031773	0.167	0.746	217.82	43.0	202.91	3.64	201.63	0.33
z17	ET2535	0.431	11	0.49	711	0.137	0.050206	0.591	0.219992	0.632	0.031780	0.078	0.570	204.54	13.7	201.90	1.16	201.68	0.15
z13	ET2535	0.331	5	0.92	302	0.106	0.050724	1.373	0.222453	1.462	0.031807	0.112	0.812	228.31	31.7	203.95	2.70	201.85	0.22
z2	ET2535	0.509	5	1.12	309	0.163	0.050405	1.260	0.221110	1.341	0.031815	0.091	0.898	213.71	29.2	202.83	2.46	201.90	0.18
z8	ET2535	0.494	2	0.88	119	0.163	0.052173	3.514	0.229776	3.744	0.031942	0.244	0.945	293.01	80.2	210.01	7.10	202.69	0.49
z14	ET2535	0.282	1	1.04	112	0.094	0.053028	4.072	0.233811	4.342	0.031978	0.291	0.932	330.02	92.4	213.34	8.36	202.92	0.58

(a) z1, z2 etc. are labels for fractions composed of single zircon grains or fragments; all fractions annealed and chemically abraded after Mattinson (2005).

(b) EARTHTIME tracer used. ET535 = 205Pb-233U-235U, ET2535 = 202Pb-205Pb-233U-235U

(c) Model Th/U ratio calculated from radiogenic 208Pb/206Pb ratio and 206Pb/238U age.

(d) Pb* and Pbc represent radiogenic and common Pb, respectively; mol % ^{206}Pb* with respect to blank Pb.

(e) Measured ratio corrected for spike and fractionation only. Mass fractionation correction of 0.25 ± 0.02 (1-sigma) %/amu (atomic mass unit) was applied to MIT North Mtn. Basalt analyses. UNIGE data corrected using either the double-Pb tracer or with 0.13±0.02 %/amu.

(f) Corrected for fractionation, spike, and common Pb; all common Pb was assumed to be procedural blank: 206Pb/204Pb = 18.39 ± 0.91%; 207Pb/204Pb = 15.45± 0.66%; 208Pb/204Pb = 37.62 ± 0.78% (all uncertainties 1-sigma). 206Pb/238U and 207Pb/206Pb ratios corrected for initial disequilibrium in 230Th/238U using Th/U [magma] = 4±1 (1-sigma).

(g) Errors are 2-sigma, propagated using the algorithms of Schmitz and Schoene (2007) and Crowley et al. (2007).

(h) Calculations are based on the decay constants of Jaffey et al. (1971).

Supplementary Table 2: composition of the EARTHTIME U-Pb tracer used in this study

205Pb	9.882260145E-12		**[mol/g]**
235U	9.902024666E-10		**[mol/g]**
235U/205Pb	100.20	0.05	**± 1σ [%]**
202Pb/205Pb	9.998900000E-01	± 0.005	**± 1σ [%]**
206Pb/205Pb	2.989385290E-04	± 0.74	**± 1σ [%]**
207Pb/205Pb	2.407104342E-04	± 0.10	**± 1σ [%]**
204Pb/205Pb	8.875074984E-05	± 0.10	**± 1σ [%]**
208Pb/205Pb	5.917328387E-04	± 0.10	**± 1σ [%]**
207Pb/206Pb	8.052171630E-01	± 0.10	**± 1σ [%]**
204Pb/206Pb	2.970280430E-01	± 0.10	**± 1σ [%]**
238U/235U	3.087000000E-03	± 0.005	**± 1σ [%]**
233U/235U	9.946400000E-01	± 0.005	**± 1σ [%]**
238U/233U	3.103635486E-03	± 0.005	**± 1σ [%]**

Eruption Ages									
	N	date	±	N (MSWD)	date	±	N (MSWD)	date	±
NMB UNIGE	1	201.34	0.11	13 (0.8)	201.37	0.02			
NMB MIT	1	201.27	0.11	19 (1.4)	201.39	0.03			
LM4-86	1	201.40	0.18	3 (0.7)	201.45	0.10	4 (3.1)	201.54	0.22
LM4-90	1	201.36	0.13	4 (0.0)	201.35	0.09	8 (0.9)	201.41	0.07
LM4-100/101	1	201.29	0.16	3 (0.4)	201.32	0.10	5 (0.3)	201.33	0.09
NYC-N10	1	201.33	0.13	3 (0.1)	201.34	0.09	10 (1.3)	201.46	0.08
Timing of Events									
age of TJB		201.31	0.18		201.33	0.11		201.36	0.12
duration of $\delta^{13}C$ excursion		0.07	+0.22/ -0.07		0.11	+0.13/ -0.11		0.08	+0.23/ -0.08

Supplementary Table 3. Estimates for eruption ages of samples from this study using different interpretations of the data. All dates are $^{206}Pb/^{238}U$ dates in millions of years. All uncertainties are at the 95% confidence interval. N = number of data points used in calculation, beginning with the youngest closed-system zircon (Fig 1C) and including the next oldest; MSWD = mean square of weighted deviates for weighted-means with N>2. Ages for events are calculated as follows: age of Triassic-Jurassic Boundary (TJB) = maximum limits of LM4-90 and minimum limits of LM4-100/101; duration of $\delta^{13}C$ excursion = age of LM4-86 - age of NYC-N10, uncertainties calculated using standard error-propagation, assuming duration cannot be <0.